

Article

Enhancement of the Surface Hydrophilicity of Poly(Vinyl Chloride) Using Hyperbranched Polylysine with Polydopamine

Yixian Zhang ^{1,2,3,*}, Dong Wang ², Ying Xu ², Li Wen ², Jian Dong ^{2,*}  and Liming Wang ^{3,*}

¹ MOE Key Laboratory of Macromolecular Synthesis and Functionalization, Department of Polymer Science and Engineering, Zhejiang University, Hangzhou 310027, China

² College of Chemistry and Chemical Engineering, Shaoxing University, Shaoxing 312000, China

³ Hisern Medical Equipment Co., Ltd., Shaoxing 312000, China

* Correspondence: yxzhang@usx.edu.cn (Y.Z.); jiangdong@usx.edu.cn (J.D.); wanglm@hisern.com (L.W.)

Abstract: In recent years, the application of polyvinyl chloride (PVC) material has significantly expanded within the realm of biomedical materials. However, the hydrophobicity of PVC has been found to cause many adverse reactions in patients within the biomedical field. It is imperative to urgently discover viable approaches for enhancing the hydrophilicity of PVC in order to ensure its safety in biomedical applications. In this study, the surface of PVC films was modified with a combination of hyperbranched polylysine (HBPL) and polydopamine (pDA) through either simultaneous deposition with polydopamine (PVC-pDA/HBPL) or successive deposition of pDA and HBPL (PVC-pDA-HBPL), aiming to investigate the influence of this modification method on surface hydrophilicity enhancement. The surface coatings were characterized using gravimetry, scanning electron microscopy (SEM), Fourier transform infrared spectroscopy (FTIR), Raman spectroscopy, and water contact angle measurements. The results demonstrated that the incorporation of HBPL led to a significant enhancement in both the deposition amount and stability of pDA, particularly when the mass ratio of DA/HBPL was approximately 1:1. Simultaneously, the morphology of the films exhibited an increase in roughness, while surface hydrophilicity was significantly enhanced upon incorporating pDA and HBPL, and the water contact angle was decreased to 43.2°. Moreover, the detachment of PVC-pDA/HBPL and PVC-pDA-HBPL after exposure to 1.0 M NaOH solutions was considerably lower compared to that of PVC-pDA alone, indicating improved stability under strongly basic conditions. Notably, these enhancements were more pronounced for PVC-pDA/HBPL than for PVC-pDA-HBPL, indicating that HBPL may act as a cross-linker during pDA deposition primarily through intermolecular Schiff base reactions, hydrogen bonding, or Michael addition. This work represents a pioneering effort in integrating HBPL and dopamine for hydrophilic modification of PVC materials, thereby expanding the potential applications of PVC materials. Additionally, we provide novel insights into constructing a hydrophilic surface based on bionic principles and expanding the potential applications of HBPL and pDA.

Keywords: poly(vinyl chloride); polydopamine; hyperbranched polylysine; surface coating



Citation: Zhang, Y.; Wang, D.; Xu, Y.; Wen, L.; Dong, J.; Wang, L. Enhancement of the Surface Hydrophilicity of Poly(Vinyl Chloride) Using Hyperbranched Polylysine with Polydopamine. *Coatings* **2024**, *14*, 103. <https://doi.org/10.3390/coatings14010103>

Academic Editor: Ludmila B. Boinovich

Received: 12 December 2023

Revised: 9 January 2024

Accepted: 10 January 2024

Published: 12 January 2024



Copyright: © 2024 by the authors. Licensee MDPI, Basel, Switzerland. This article is an open access article distributed under the terms and conditions of the Creative Commons Attribution (CC BY) license (<https://creativecommons.org/licenses/by/4.0/>).

1. Introduction

Medical plastics have garnered significant attention due to their cost efficiency, high production capacity, and wide market demand. Among them, poly(vinyl chloride) (PVC) stands out as one of the most extensively utilized polymers owing to its commendable chemical stability, exceptional mechanical strength, and ease of production. PVC has found widespread application in the medical field, encompassing various medical hoses, blood storage devices, dialysis accessories, surgical gloves, artificial organs, and more [1]. However, the hydrophobic nature of PVC poses new challenges such as undesired cell and protein adhesion as well as tissue damage upon introduction into the human body. Consequently, there is an urgent need to enhance the surface hydrophilicity of PVC while simultaneously improving its safety for biomedical applications.

It is widely recognized that *mytilus edulis* exhibits remarkable strength and surface lubricity in water, which can be attributed to the presence of mytilus foot protein (Mtp) in the byssal gland on its surface [2–4]. The hydrolysis product of Mtp has been identified primarily as 3,4-dihydroxy-L-phenylalanine (DOPA), lysine, and hydroxyproline residues [5]. For instance, approximately 27% of DOPA residues and 15% of lysine residues were detected in the amino acid sequence of Mtp-5, which are considered the primary factors contributing to the adhesion and lubricity properties of Mtp [6,7]. Owing to their exceptional adhesive characteristics, mussel-inspired polydopamine (pDA) coatings have gained significant attention in various fields such as biomedicine [8,9], national defense [10], and marine engineering [11,12] over recent years. Dopamine (DA), also referred to as catecholamine or trihydroxytyramine, with a structure of $C_6H_3(OH)_2-CH_2-CH_2-NH_2$, is an intermediate product of tyrosine metabolism and commonly utilized in the form of dopamine hydrochloride. Under weakly alkaline conditions, pDA can be spontaneously formed through dopaminergic oxidation, self-polymerization, and cross-linking reactions [13–15]. The deposition of DA on various substrates has been investigated, providing a platform for subsequent grafting with multiple functional groups [16–18]. However, the instability of pDA coatings in alkaline solutions and organic solvents, particularly polar solvents, poses a challenge for their practical application in secondary grafting [19,20]. For instance, Wei [21] reported that PDA-coated substrates such as polypropylene (PP), poly(vinylidene fluoride) (PVDF), and nylon exhibited remarkable stability in strongly acidic solutions; however, the detachment percentage significantly increased in 1.0 M NaOH. Therefore, it is imperative to enhance the chemical stability of PDA coatings to serve as a reliable platform for secondary grafting. Nonetheless, there are limited amino groups available for secondary grafting after dopamine self-polymerization [22–24]. Consequently, it would be ideal if we could achieve both sufficient functional group preservation for secondary grafting and enhanced stability of the pDA coatings.

In recent years, numerous studies have been reported focusing on enhancing the hydrophilicity of PVC surfaces. Kathryn [25] demonstrated a physisorbed free radical chain transfer grafting technique to initiate the polymerization of hydrophilic monomers through the physisorption of a hydrophobic initiator onto the PVC surface. Additionally, composite hydrogel paints (CHPs) consisting of zwitterionic copolymers or microgels were employed to effectively improve the hydrophilicity of PVC to prevent thrombus formation in PVC intervention materials [26]. Furthermore, an effective approach to enhance hydrophilicity involves implanting nanoparticles (NPs), such as TiO_2 -NPs, onto PVC surfaces where TiO_2 -NPs serve as agents for hydrophilic modification [27]. Ahmad [28] demonstrated a significant enhancement in the hydrophilicity of PVC film when incorporating acrylamide-grafted bentonite, which exhibited excellent antifouling properties for oil/wastewater separation.

Simultaneously, when modifying a material surface to be hydrophilic, it is crucial to consider the durability of these coatings. Zhao [29] successfully developed a stable copper nanowire composite film by introducing a pDA-modified alginate matrix, resulting in an exceptionally smooth surface with remarkable interface adhesion. Various types of oxidants (e.g., $CuSO_4/H_2O_2$ [30], $(NH_4)_2S_2O_8$ [31], and $NaIO_4$ [32]) can be utilized during pDA polymerization to enhance covalent interactions and improve the stability of pDA coatings. However, this method requires increased consumption of amino groups during the DA cyclization reaction, which may not be advantageous for secondary grafting purposes.

Generally speaking, ϵ -poly-L-lysine (ϵ -PL) or α -poly-L-lysine (PLL) can be synthesized through the polymerization of L-lysine using different synthetic approaches [33]. Among the various types of polylysine, hyperbranched polylysine (HBPL) is a widely distributed and randomly branched polymer containing both ϵ -PL and PLL units. With its highly branched structure and abundant terminal amines, HBPL is well-suited for secondary grafting and modification. Yang [34] successfully immobilized HBPL onto a titanium substrate to achieve antibacterial, anti-inflammatory, and osteogenic functions. Additionally, surface modification with PLL has been reported to neutralize the charge of extracellular matrix

surfaces, thereby inhibiting cell and tissue adhesion to prevent postoperative adhesions [35]. Yuan [36] also demonstrated that modifying poly(lactic-co-glycolic acid (PLGA) microspheres with PLL can impart excellent protein-repellent properties, which is conducive to cell adhesion. However, there have been few studies focused on the applications of HBPL in surface hydrophilic modification.

Inspired by hydrolysis product components of Mtps, pDA alone and pDA coupled with HBPL were investigated to enhance the surface hydrophilicity of PVC. HBPL was synthesized via melt phase polycondensation and characterized using ^1H nuclear magnetic resonance ($^1\text{HNMR}$), Fourier transform infrared (FTIR) spectra, Raman spectroscopy, and gel permeation chromatography (GPC). To determine the optimal approach for surface modification, HBPL was either co-deposited with pDA (PVC-pDA/HBPL) or covalently grafted onto pDA-deposited PVC (PVC-pDA-HBPL). The stability of these coatings was evaluated by examining their surface morphology and water contact angle after elution with 1.0 M HCl and 1.0 M NaOH, which represent strong acid and alkali conditions, respectively. There has been extensive research conducted in the past regarding the hydrophilic modification of PVC material surfaces. However, this study represents a novel approach by employing HBPL and pDA to enhance the surface wettability of PVC materials. This study provides new insights into constructing a hydrophilic surface based on bionic principles while expanding the application potential of HBPL and pDA. Additionally, the reported antibacterial effect of HBPL [37] suggests the potential for further investigation into enhancing the antibacterial properties of PVC materials in future research.

2. Materials and Methods

2.1. Materials

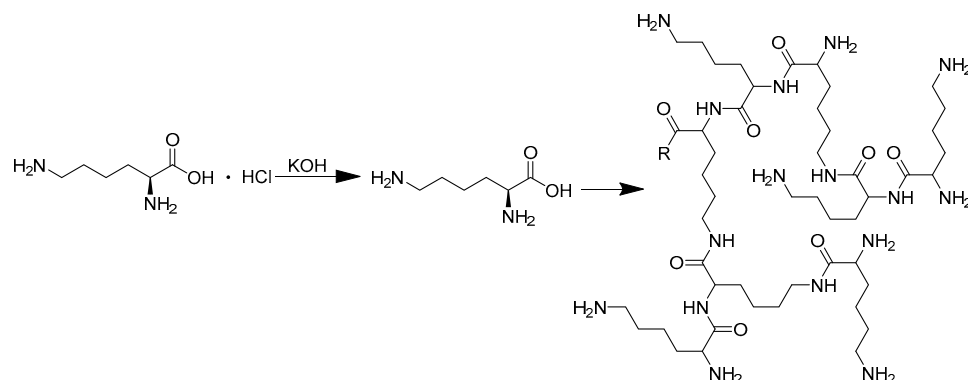
Dopamine hydrochloride, potassium hydroxide, and methanol were purchased from Aladdin Chemistry Co., Ltd., Shanghai, China. Lysine hydrochloride was purchased from Tokyo Chemical Industry, Tokyo, Japan. Zirconium n-butoxide was purchased from Admas Chemistry Co. Ltd., Shanghai, China. Tris-(hydroxymethyl)aminomethane (Tris) was purchased from Beyotime Biotechnology, Haimen, China. All chemicals were of analytical grade and used as received if not specifically stated otherwise. Milli-Q water (Merck, Rahway, NJ, USA) was used throughout the experiments. PVC was obtained from Zhejiang Haisheng Medical Device Co., Ltd., Shaoxing, China.

2.2. Preparation of Hyperbranched Polylysine

The hyperbranched polylysine utilized in this experiment was synthesized following the previously reported procedure [38] illustrated in Scheme 1. In brief, a mixture of 54.8 g L-lysine hydrochloride and 16.8 g KOH was thoroughly blended in a three-neck flask and subjected to a 2 h reaction with mechanical stirring. Subsequently, the system was heated to 150 °C until the hybrid transformed into a molten state. A catalyst of 7.2 mL $\text{Zr}(\text{O}^n\text{Bu})_4$ (equivalent to 3 mol% of the lysine monomer) was added, and the reaction proceeded for 8 h under nitrogen protection with an open state for water evaporation. The resulting brown samples were dissolved in 200 mL methanol, and the KCl byproduct was eliminated through centrifugation at $6500\times g$ for 15 min. Finally, methanol was removed via spin evaporation. The product was redissolved in methanol and dialyzed against water using a dialysis bag with a molecular weight cutoff of 3500 for three days. HBPL was refined through freeze-drying, resulting in a yellowish product with an average molecular weight of approximately 6.2 kDa and a molecular weight distribution index of 1.74, as determined by means of GPC (1260 Infinity II, Agilent, Santa Clara, CA, USA).

The structure of HBPL was confirmed through $^1\text{HNMR}$ spectroscopy, utilizing a Bruker DMX500 (Bruker, Billerica, MA, USA) instrument operating at 500 MHz with D_2O as the solvent and tetramethylsilane as the reference compound. Fourier transform infrared (FTIR) spectra were obtained using KBr pellets on a NICOLET6700 instrument (Thermo Fisher Scientific, Waltham, MA, USA). Additionally, the Raman spectra were obtained using a Raman microscope (DXR3, Thermo Fisher Scientific, Waltham, MA, USA) equipped

with a 785 nm solid-state laser (20 mW), 50×/0.75 numerical aperture (NA) objective lens, Renishaw CCD detector, and Olympus microscope. Exposure time was 10 s, and spectral resolution was 0.5 cm⁻¹.



Scheme 1. The HBPL synthesis diagram.

2.3. pDA/HBPL Co-Deposition on PVC

A PVC film (1.5 cm × 1.5 cm × 0.155 mm) was subjected to three rounds of sonication with ethanol and distilled water for washing purposes. Subsequently, the PVC film was immersed in a solution containing DA/HBPL in Tris-HCl buffer solution (50 mM, pH = 8.5) within a 15 mL vessel and shaken at room temperature (23 ± 2 °C) for a duration of two days using a shaking incubator. To investigate the influence of HBPL mass proportion on the stability of pDA/HBPL, parallel experiments were conducted using varying ratios of DA/HBPL: 4:1, 2:1, 1:1, 0:1, 1:2, 1:4, and 1:0 (with both DA concentrations set at 2 mg/mL). Finally, the modified samples were washed thrice with ethanol and then with distilled water before being dried at an oven temperature of 50 °C. These samples were designated as PVC-pDA/HBPL. The deposition density (DD) on the substrate materials was calculated based on the following formula:

$$DD = (m_1 - m_0)/S, \quad (1)$$

where m_0 and m_1 are the mass of the substrate material before and after deposition (mg), and S is the area of the substrate material. The mass of the substrate material before and after deposition was measured using electronic analytical balance.

2.4. Successive Deposition of pDA and HBPL on PVC

The successive deposition of pDA and HBPL onto PVC was conducted following a similar procedure. Firstly, PVC films were treated with a 2 mg/mL DA solution for 2 days until the films turned brown in color. Subsequently, the films were washed three times with ethanol and water to remove physically adsorbed pDA, followed by drying in a sealed oven at 50 °C for subsequent experiments. To achieve adequate dissolution, HBPL in varying concentrations (where the mass ratio of HBPL to the previously added DA was 4:1, 2:1, 1:1, 0:1, 1:2, 1:4, or 1:0) was added into the Tris-HCl buffer and stirred at room temperature (23 ± 2 °C) for two hours. pDA-coated PVC films were then immersed individually into the corresponding solutions. The beaker containing the film was sealed with plastic wrap and placed in an oven at 50 °C for two days to allow sufficient grafting of HBPL onto the surface. Finally, the film was removed from the solution and cleaned three times with deionized water before being vacuum-dried overnight at 50 °C to obtain the PDA–HBPL successively modified film named PVC-PDA-HBPL.

2.5. Surface Modification Measurement

An attenuated total reflection infrared spectrometer (ATR-FTIR, NEXUS, Thermo Fisher Scientific, Waltham, MA, USA) equipped with a germanium crystal accessory was

employed to investigate the surface structural modifications of the samples. The Raman spectrum of the films was analyzed using the same methodology as described in Section 2.1. The measured wavenumber range spanned from 4000 cm^{-1} to 600 cm^{-1} at a resolution of 4 cm^{-1} with 32 scans. To elucidate their morphology, the samples were sputtered with gold and subjected to analysis using scanning electron microscopy (SEM, JSM-6360LV, JEOL, Tokyo, Japan). The elemental composition of the samples at a specific location was determined using energy-dispersive X-ray spectroscopy (EDS, QX200, Bruker, Leipzig, Germany). Atomic force microscopy (AFM, Bruker Multimode 8, Columbus, OH, USA) was used to evaluate surface roughness.

Contact angles were determined using an automated single-fiber contact angle goniometer (OCA50 micro, Dataphysics, Filderstadt, Germany) equipped with video capture functionality within a controlled environmental chamber. A precisely measured $3\text{ }\mu\text{L}$ droplet of filtered and deionized distilled water was carefully deposited onto the surface of the samples at ambient temperature. The contact angles were subsequently measured after allowing for the samples to stabilize for a duration of 1 min. Each reported value represents the average obtained from five independent measurements.

2.6. Evaluation of the Stability of the Surface Coating

To assess the stability of the sample under harsh acidic and alkaline conditions, PVC-PDA/HBPL and PVC-PDA-HBPL were subjected to a 1.0 M HCl or a 1.0 M NaOH solution for a duration of 2 h, while the elution was monitored using a UV-visible spectrophotometer (UV-2600, Hewlett Packard, Palo Alto, CA, USA). The surfaces of the eluted samples were subsequently characterized using SEM analysis and water contact angle measurements. Additionally, fresh 1.0 M HCl or 1.0 M NaOH solutions were employed every 2 h to replace the eluent, with the absorbance at 280 nm being measured in each case. In addition, the eluted samples were carefully weighed, and the remaining DD of PVC film was subsequently determined using the method described in Section 2.3 to accurately assess the quantitative impact of acid-base treatment on coating adhesion.

2.7. Confirmation of the Reaction between HBPL and DA

To gain insights into the specific reaction mechanism of HBPL and DA on the surface of PVC film, a comparative study was conducted in Tris-HCl solution (50 mM, pH = 8.5) to mimic their interaction. Specifically, 2 mg/mL of either DA or a mixture of DA and HBPL (mass ratio = 1:1) was separately introduced into the Tris-HCl solution and incubated under sealed conditions at room temperature ($23 \pm 2\text{ }^\circ\text{C}$) for 48 h. The product underwent a three-day dialysis process in water using a dialysis bag with a molecular weight cutoff of 3500. Subsequently, freeze-drying was performed, followed by characterization using FTIR and Raman spectroscopy to elucidate the reactions between HBPL and DA under identical conditions but in the absence of PVC film.

2.8. Statistical Analysis

The data are presented as the mean \pm standard deviation, with 4 to 6 samples examined in parallel for all experiments. The statistical significance of differences between groups was determined using one-way analysis of variance (ANOVA) in Origin 2021 software. The Tukey Means Comparison method was employed, and statistical significance was defined at $p < 0.05$.

3. Results and Discussion

3.1. Characterization of HBPL

HBPL was synthesized through melt phase polycondensation using an open system reaction, where the water byproduct was evaporated. The structure of HBPL was confirmed via ^1H NMR spectroscopy, as shown in Figure 1 (^1H NMR (500 MHz, D_2O): δ 3.29–4.20 (t, 2H), 2.81–3.34 (m, 4H), 1.17–1.71 (m, 12H)). These results demonstrate the successful synthesis of HBPL.

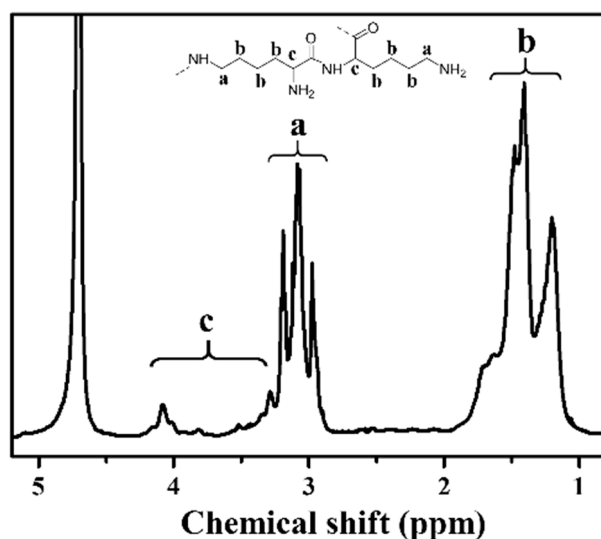


Figure 1. ^1H NMR spectrum of HBPL (a, b, and c denote the chemical shifts corresponding to distinct hydrogen species in HBPL).

3.2. Characterization of the Coated Surface

3.2.1. Morphology and Deposition Behavior

Deposition density of the various prepared surfaces was assessed by comparing the weight of the films before and after modification, as presented in Table 1. The adhesion of HBPL to PVC films was found to be challenging without the synergistic effect of pDA. Furthermore, compared with that on other reported polymer surfaces such as PP and PTFE, the deposition density of pDA on PVC film was relatively low [39]. Overall, it was observed that the deposition density for PVC-pDA/HBPL was of a higher magnitude compared to that for PVC-pDA-HBPL, suggesting that co-deposition offered greater advantages in terms of achieving higher quantities of deposition as opposed to the successive deposition method. In contrast, deposition density reached its maximum when the mass ratio of DA/HBPL was 1:1 (approximate stoichiometric ratio of 1.17) for both samples. For PVC-pDA/HBPL, this could be attributed to HBPL playing a crucial cross-linking role in the coating process. However, exceeding the optimal amount of HBPL resulted in a decrease in coating quantity due to a decline in pDA deposition. Therefore, based on these findings, we selected a ratio of 1:1 for subsequent experiments.

Table 1. Deposition density values (mg/cm^2) for PVC-pDA/HBPL and PVC-pDA-HBPL with different mass ratios of DA/HBPL.

Sample	DA/HBPL Ratio						
	4:1	2:1	1:1	0:1	1:2	1:4	1:0
PVC-pDA/HBPL	0.034 ± 0.004	0.038 ± 0.010	0.043 ± 0.009	0.001 ± 0.003	0.027 ± 0.006	0.022 ± 0.008	0.021 ± 0.003
PVC-pDA-HBPL	0.023 ± 0.004	0.029 ± 0.005	0.031 ± 0.003	0 ± 0.002	0.029 ± 0.011	0.031 ± 0.007	0.021 ± 0.003

The color of the PVC substrate and pDA-HBPL- or pDA/HBPL-deposited samples exhibited noticeable changes, as depicted in the inset of Figure 2. Initially, the PVC membrane possessed a colorless and transparent appearance; however, upon deposition with pDA, it transformed to a light grey shade with slightly reduced transparency. Irrespective of whether pDA/HBPL co-deposition (PVC-pDA/HBPL) or consecutive modification by pDA and HBPL (PVC-pDA-HBPL) was performed, both approaches exhibited a discernible transition towards a light brown hue. This observed color transformation unequivocally signifies the efficacy of pDA deposition, as well as the active involvement of HBPL during DA polymerization for co-deposition (PVC-pDA/HBPL) or successful modification onto PVC-pDA surfaces.

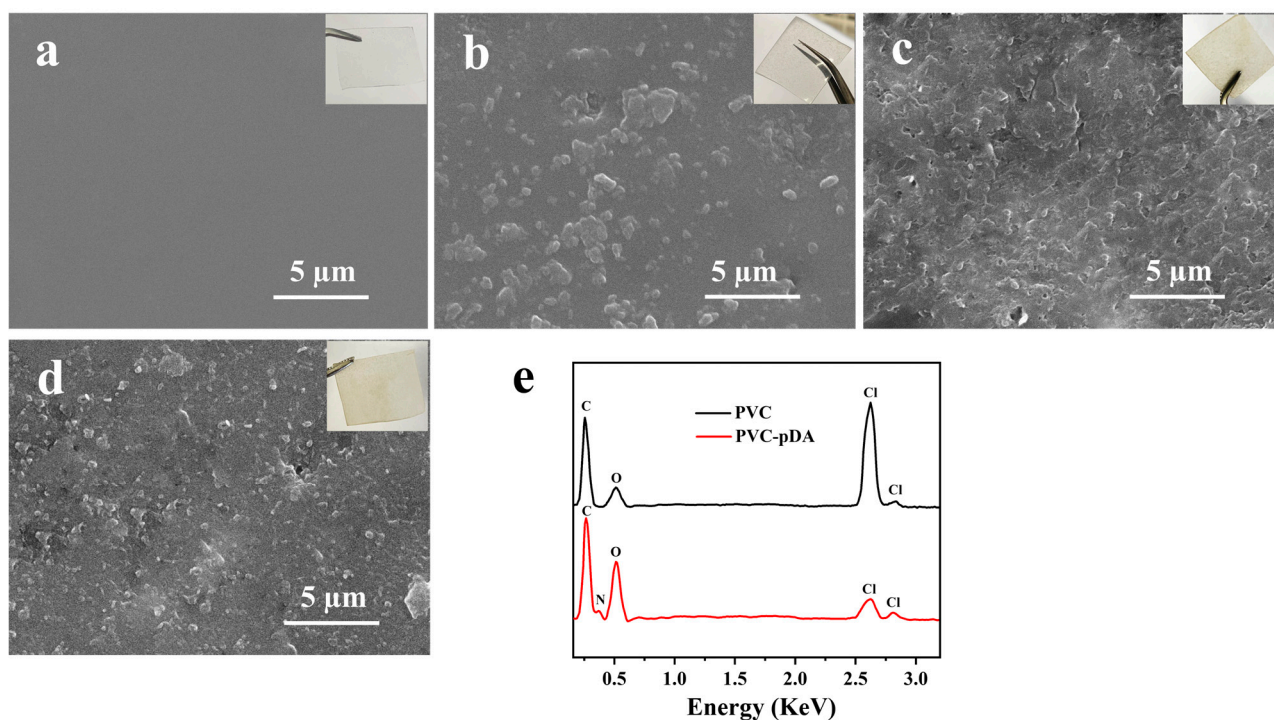


Figure 2. SEM images (insets are the corresponding photographs) of (a) PVC, (b) PVC-pDA, (c) PVC-pDA/HBPL, (d) PVC-pDA-HBPL; and (e) EDS spectrum of pristine PVC and PVC-pDA.

It has been reported that pDA can readily aggregate and deposit on various surfaces through non-covalent interactions such as hydrogen bonding and π - π stacking [40]. SEM images (Figure 2b) clearly show the presence of granular stuff on the PVC films' surface. Based on elemental analysis results obtained through energy-dispersive X-ray spectroscopy (EDS) of PVC film and dot scanning of particles on PVC-pDA surface (Figure 2e), it was observed that the present particles exhibited a distinct nitrogen signal, suggesting their predominant composition as pDA aggregates. The deposition of pDA aggregates onto the PVC surface imparts a gray hue to the sample. However, the surficial deposits exhibited increased weight and complexity when HBPL was involved in conjunction with pDA (Figure 2c,d). This can be attributed to the covalent interaction between HBPL and pDA, which consequently weakens the non-covalent interactions among pDA molecules, leading to the formation of complex co-deposits on PVC substrates, aligning with previous research findings [41]. pDA particles decreased noticeably when PVC-pDA/HBPL and PVC-pDA-HBPL were introduced, being replaced by the accumulation of wrinkle- or mash-like substances, which are most likely HBPL polymers. This phenomenon was more pronounced in the case of PVC-pDA/HBPL compared to PVC-pDA-HBPL, suggesting that co-deposition favored HBPL modification, possibly due to the interference effect of HBPL on pDA deposition [42]. The presence of the pDA aggregate and yellowish HBPL on the surface of PVC film imparted a light brown hue to the film. These findings align with the results obtained for deposition density, as presented in Table 1.

In addition, the surface roughness before and after modification was determined using atomic force microscopy (AFM), as shown in Figure 3. It is evident from Figure 3b–d that PVC-pDA, PVC-pDA/HBPL, and PVC exhibited a higher degree of surface roughness compared to pure PVC. Correspondingly, the root mean squared area roughness (Sq) of the PVC increased significantly from 7.5 ± 1.4 nm to 21.1 ± 2.5 nm upon coating with pDA, and it further escalated to 32.2 ± 1.8 nm and 29.5 ± 2.1 nm following modification with pDA/HBPL and pDA-HBPL, respectively, which can be attributed to the grafting of polymer particulates onto the surface.

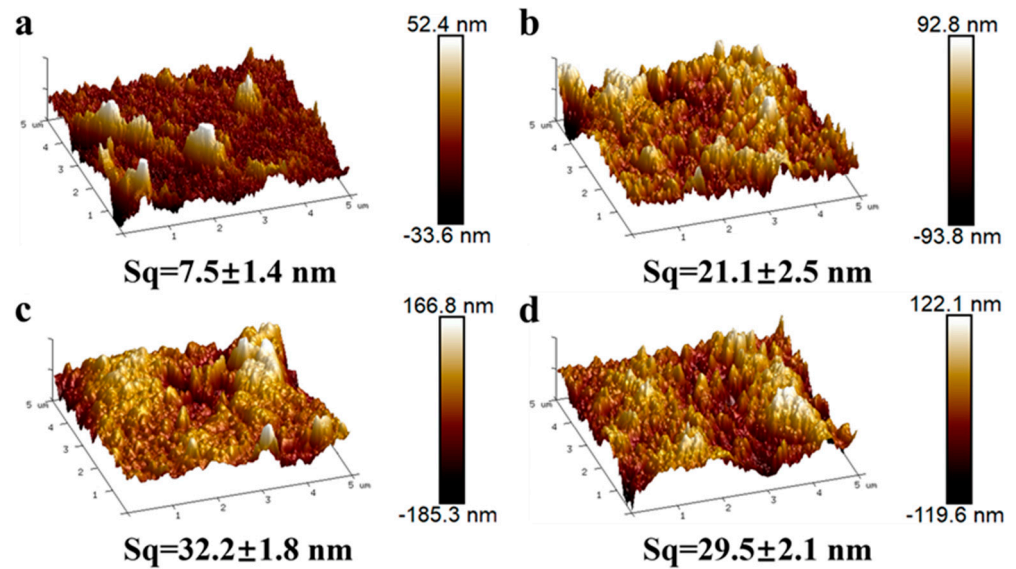


Figure 3. Three-dimensional maps characterizing the AFM results for (a) PVC, (b) PVC-pDA, (c) PVC-pDA/HBPL, and (d) PVC-pDA-HBPL. The variable S_q denotes the root mean square of surface roughness in the given area.

3.2.2. FTIR and Raman Spectroscopy

The overlaid FTIR spectra of HBPL and ATR-FTIR spectra of uncoated PVC, PVC-pDA, PVC-pDA/HBPL, and PVC-pDA-HBPL are depicted in Figure 4a. As illustrated in Figure 4a, the spectrum exhibits distinct absorption peaks at 1637 cm^{-1} and 1530 cm^{-1} , corresponding to the stretching vibration peak of $\text{C}=\text{O}$ on the amide bond and the coupling of N-H bending vibration and $\text{C}=\text{O}$ stretching vibration, respectively. Furthermore, the absorption peaks observed at 3280 cm^{-1} and 1265 cm^{-1} can be attributed to the stretching vibrations of amide group N-H and C-N bonds, providing further evidence for the successful synthesis of HBPL. The spectra of the surfaces modified with pDA and HBPL exhibit a broad absorption peak at 3300 cm^{-1} , corresponding to the presence of $-\text{OH}$, $-\text{NH}$, and $-\text{NH}_2$ groups from pDA or HBPL. In the PVC-pDA, PVC-pDA/HBPL, and PVC-pDA-HBPL spectra, emerging peaks at 1560 cm^{-1} and 1645 cm^{-1} were observed due to the vibration of the benzene ring structure in DA, indicating successful deposition of pDA. Notably, a new absorption peak at 1652 cm^{-1} was detected in the spectra of PVC-pDA/HBPL and PVC-pDA-HBPL, attributed to $\text{C}=\text{N}$ stretching vibration, suggesting successful modification of PVC with pDA/HBPL wherein HBPL might be covalently linked with DA through a Schiff base reaction.

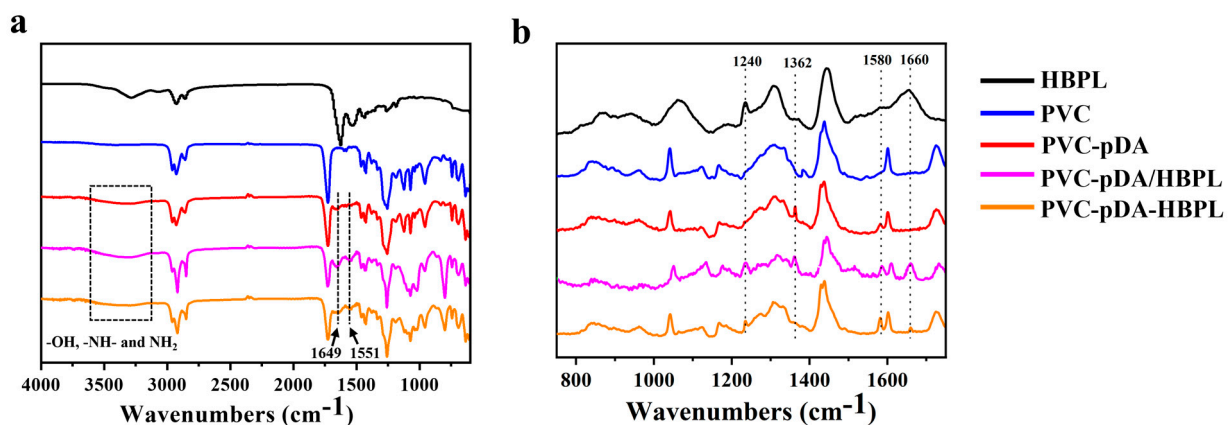


Figure 4. (a) FTIR or ATR-FTIR and (b) Raman spectra of different samples.

Additionally, Raman spectroscopy was employed to investigate the alterations in surface properties of various modified samples pre and post modification (Figure 4b). It showed that the formation of pDA primarily relies on hydrogen bonding and π - π interaction, resulting in the development of a graphene-like structure. Upon comparing the Raman spectra of PVC and PVC-pDA, it is evident that novel peaks emerge at 1362 cm^{-1} and 1580 cm^{-1} , corresponding to the aromatic structures in pDA, signifying the successful deposition of pDA onto the surface of PVC. In addition, for PVC-pDA/HBPL and PVC-pDA-HBPL, the presence of the amide bond peaks at 1240 cm^{-1} and 1660 cm^{-1} indicates successful modification with HBPL.

3.2.3. Surface Wettability

The wettability of the modified PVC films was characterized using water contact angle measurements, yielding an average value derived from the left and right contact angles (Figure 5). The water contact angle of pristine PVC was approximately 108° , indicating its hydrophobic properties. However, this value significantly decreased after surface modification with pDA and was further reduced upon deposition of pDA/HBPL and pDA-HBPL coatings. This observation clearly demonstrates that the introduction of HBPL enhanced the hydrophilicity of pDA coatings. Moreover, it is noteworthy that the surface wettability of pDA/HBPL surpassed that of PVC-pDA-HBPL, which aligns with the deposition density results and suggests that the co-deposition method outperforms successive grafting in terms of improving surface characteristics. The hydrophilic coating achieved through this straightforward treatment method exhibited a significantly enhanced hydrophilicity compared to that obtained via conventional coating [43] or blending techniques [44]. These findings confirm our hypothesis regarding the ability of HBPL to optimize pDA deposition behavior and enhance surface hydrophilicity.

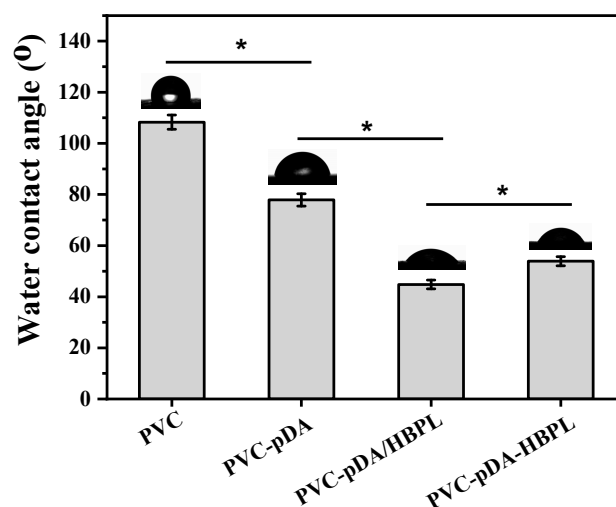


Figure 5. Water contact angles of unmodified and modified PVC substrates. * indicates significant difference at $p < 0.05$ level.

3.3. Stability of Coatings after Elution

3.3.1. Surface Morphology Changes

The introduction of HBPL resulted in enhanced deposition of pDA and improved surface wettability. If these surface coatings can also exhibit stability, they hold great promise as a hydrophilic modification alternative for PVC materials. As depicted in Figure 6, substrates coated with pDA, pDA/HBPL, or pDA-HBPL exhibited distinct changes after elution with 1.0 M HCl and NaOH. The morphologies of these samples showed minimal differences compared to the pristine surface in Figure 2 after elution with 1.0 M HCl, indicating that the involvement of pDA and HBPL allowed for stable performance even under strongly acidic conditions.

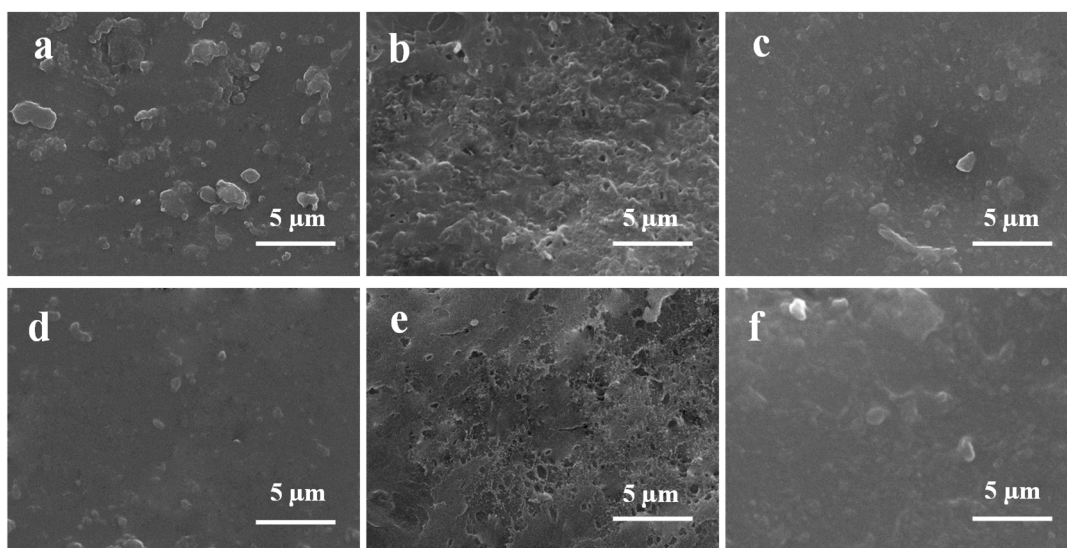


Figure 6. SEM images of (a,d) PVC-pDA, (b,e) PVC-pDA/HBPL, and (c,f) PVC-pDA-HBPL eluted with 1.0 M HCl (a–c) or 1.0 M NaOH solution (d–f) for 24 h.

However, upon elution with 1.0 M NaOH, a visual reduction in aggregates was observed, shown in Figure 6d, for PVC-pDA membranes, suggesting the instability of the pDA coating when exposed to strongly basic conditions. In contrast, the morphology of PVC-pDA/HBPL and PVC-pDA-HBPL remained relatively stable. However, a noticeable increase in surface roughness was observed in PVC-pDA/HBPL, suggesting that some un-cross-linked pDA aggregates may have been washed away by the NaOH solution. In conclusion, the surface coating comprising pDA and HBPL exhibited excellent resistance to acidic conditions; however, under strongly basic conditions, the stability of pDA deposition was compromised. Interestingly, this instability could be enhanced through the incorporation of HBPL as it acted as a cross-linker for pDA and facilitated surface modification.

3.3.2. The Detachment of Coatings after Elution

To investigate the long-term durability of the modified surfaces against harsh acids and alkalis, the films were immersed in a solution containing strong acid or alkali, with regular replacement of the cleaning solution every two hours. Given the pronounced ultraviolet absorption at 280 nm of pDA, the variation in ultraviolet absorption of the eluent at this wavelength was assessed to determine the stability of the coated surfaces after several rounds of elution with strong acid and base solutions. The results are depicted in Figure 7.

As shown in Figure 7a, the absorbance of the eluent obtained from all films subjected to washing with a 1.0 M HCl or a 1.0 M NaOH solution exhibited a rapid decrease, reaching a threshold after the initial washing step. This observation suggests that detachment of both pDA and pDA/HBPL coatings primarily took place within the first two hours of elution. Furthermore, it was observed that during the initial two-hour period, the absorbance of the eluent in the 1.0 M NaOH solution was much higher compared to that in the 1.0 M HCl solution, indicating greater stability of the pDA coating and the pDA/HBPL coating in acidic conditions rather than alkaline conditions. Notably, when the pDA/HBPL coating was immersed for two hours in a 1.0 M NaOH solution, the absorbance of its eluent was lower than that of an eluent from the pDA coating, suggesting enhanced stability of the pDA coating upon the introduction of HBPL under strongly alkaline conditions. This phenomenon was more pronounced for PVC-pDA/HBPL compared to PVC-pDA-HBPL, providing additional evidence supporting the favorable effect of co-deposition on enhancing the stability of pDA coatings.

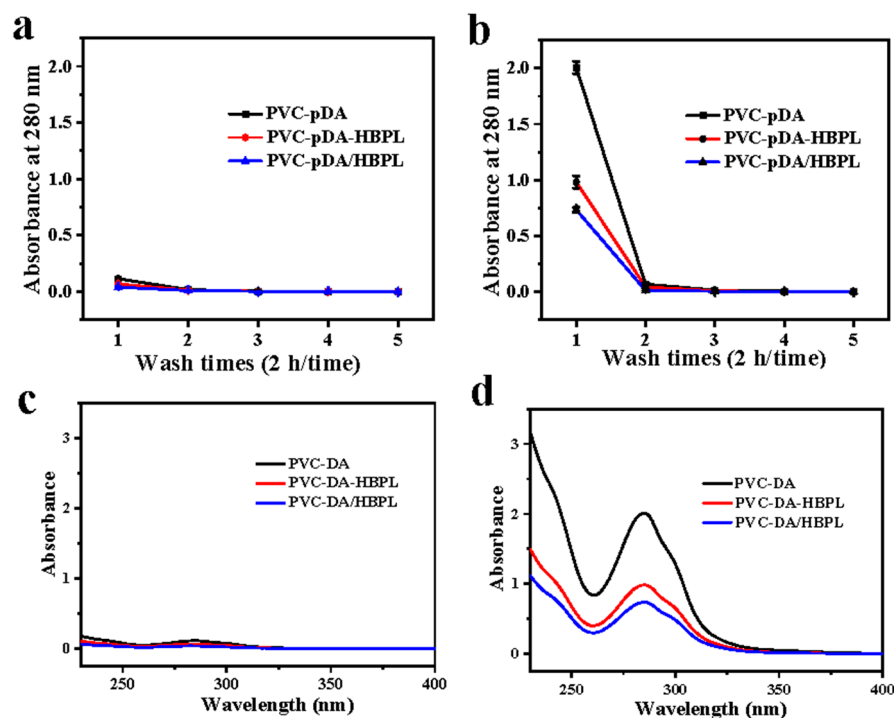


Figure 7. (a,b) Absorbance at 280 nm of eluent from modified samples during repeated elution (2 h/time) with (a) 1.0 M HCl or (b) 1.0 M NaOH solution ($n = 4$). (c,d) UV-vis spectra of the eluent of modified materials immersed in (c) 1.0 M HCl or (d) 1.0 M NaOH solution for 2 h.

To assess the quantitative impact of acid or base treatment on detachment of the PVC coating, the DD before and after elution was evaluated, as shown in Table 2. The DD values of the three coatings did not exhibit significant changes following treatment with 1.0 M HCl, which is consistent with the findings from SEM and UV-vis analysis of the eluent, thereby further confirming their excellent stability in an acidic environment. Subsequently, upon treatment of the pDA coating with 1.0 M NaOH, a nearly 50% decrease in DD was observed, indicating that pDA can be easily eluted by alkaline solutions and exhibits poor stability under such conditions. Conversely, only a slight reduction in DD was observed for both the pDA/HBPL and PDA-HBPL coatings when exposed to an alkaline solution, highlighting that the incorporation of HBPL significantly enhanced the resistance of these coatings against alkali-induced degradation. The observed enhancement in the stability of HBPL surpasses that reported for PEI [39], suggesting superior reactivity of HBPL and pDA.

Table 2. The deposition density values (mg/cm^2) of PVC-pDA, PVC-pDA/HBPL, and PVC-pDA-HBPL before and after elution with 1.0 M HCl and 1.0 M NaOH for 24 h.

Sample	Uneluted	Eluted with HCl	Eluted with NaOH
PVC-pDA	0.021 ± 0.003	0.020 ± 0.001	0.011 ± 0.002
PVC-pDA/HBPL	0.043 ± 0.009	0.042 ± 0.004	0.037 ± 0.005
PVC-pDA-HBPL	0.031 ± 0.003	0.029 ± 0.002	0.025 ± 0.003

3.3.3. Water Contact Angle Changes

Subsequently, the hydrophilicity of the substrates was evaluated by characterizing the changes in water contact angle before and after elution for 2 h. As depicted in Figure 8, no significant alteration in the water contact angle was observed for any of the substrates after elution with 1.0 M HCl, which is consistent with the SEM images presented in Figure 6a–c. However, a remarkable increase in water contact angle was observed for PVC-pDA following elution with 1.0 M NaOH, further confirming the detachment of pDA aggregates under strongly basic conditions, as demonstrated in Figure 6d.

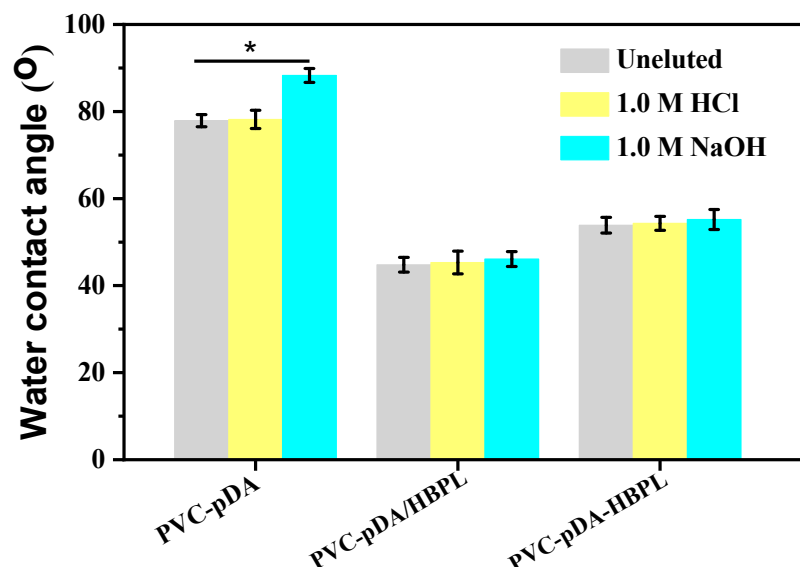


Figure 8. Water contact angles of PVC-pDA, PVC-pDA/HBPL, and PVC-pDA-HBPL after elution with 1.0 M HCl or 1.0 M NaOH solution for 2 h. * indicates significant difference at $p < 0.05$ level.

After elution with 1.0 M NaOH for 2 h, the water contact angles of the pDA/HBPL and pDA-HBPL coatings exhibited minimal change, further supporting the notion that incorporating HBPL could enhance the alkali resistance of deposited pDA. Generally, pDA coatings demonstrated relative stability in acidic solutions but could be detached using a 1.0 M NaOH solution. However, this instability was effectively mitigated by introducing HBPL. The co-deposited HBPL primarily acted as a cross-linker for pDA, thereby improving its stability. Simultaneously, HBPL grafted onto PVC-pDA functions as a robust protective layer, ensuring the integrity of the deposited pDA [45] and enabling the surface to maintain its hydrophilicity even under strongly alkaline conditions. After the incorporation of HBPL into the coating, the stability of the surface modification was significantly enhanced in comparison to that reported in the literature [46].

3.4. Confirmatory Reaction between HBPL and DA

To investigate the bonding mode of pDA and HBPL, the lyophilized products obtained after the reaction between DA and HBPL were characterized using FTIR and Raman spectroscopy (Figure 9). In Figure 9A, absorption peaks at 3347 cm^{-1} and 1288 cm^{-1} correspond to the N-H stretching vibration and the C-O stretching vibration of the phenolic hydroxyl group in pDA, respectively. The presence of a distinct absorption peak at 2938 cm^{-1} , corresponding to the C-H stretching vibration in HBPL, indicates the successful incorporation of HBPL into pDA-HBPL. Additionally, a new absorption peak emerged at 1658 cm^{-1} , corresponding to the formation of Schiff base bonds through C = N interactions. These findings suggest that HBPL primarily connects with pDA through hydrogen bonding and Schiff base bond formation.

The Raman spectral results for the reaction products from pDA and pDA/HBPL are presented in Figure 9B. The Raman spectrum of pDA once again confirms the presence of an aromatic structure, corresponding to the peaks at 1357 cm^{-1} and 1576 cm^{-1} , which aligns with the findings from surface deposition as discussed in Section 3.2.3. Additionally, the amide bands at 1257 cm^{-1} and 1440 cm^{-1} observed in pDA/HBPL correspond to the amide bonds present in HBPL. Notably, a new peak at 1663 cm^{-1} is attributed to the C = N band within the Schiff base, further substantiating that HBPL and pDA can be covalently linked through Schiff base bonds.

Combined with the aforementioned results for surface grafting and solution reaction products, the binding effect of pDA or pDA/HBPL on PVC films can be inferred, as illustrated in Figure 10. The presence of NH_2 or -OH groups in pDA leads to its positive or

negative charge in strongly acidic or alkaline conditions, resulting in electrostatic repulsion and subsequent detachment of oligomer in the pDA coating, exhibiting particularly extreme instability in strong bases. However, HBPL acts as a cross-linker during pDA deposition primarily through intermolecular Schiff base reactions, hydrogen bonding, and Michael addition, which has also been claimed in previous studies [38,47]. Due to this cross-linking role, the addition of HBPL further enhances the stability of surface modification.

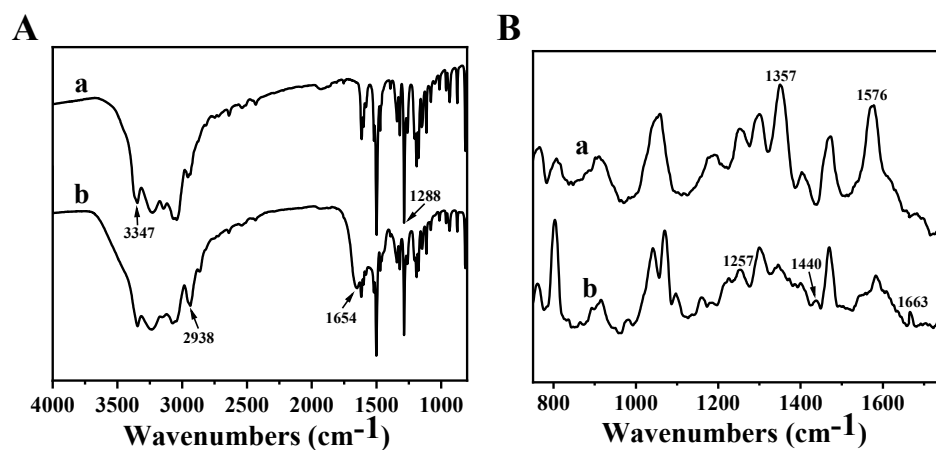


Figure 9. (A) FTIR and (B) Raman spectra of (a) pDA and (b) pDA/HBPL acquired from a solution-based reaction in the absence of PVC film.

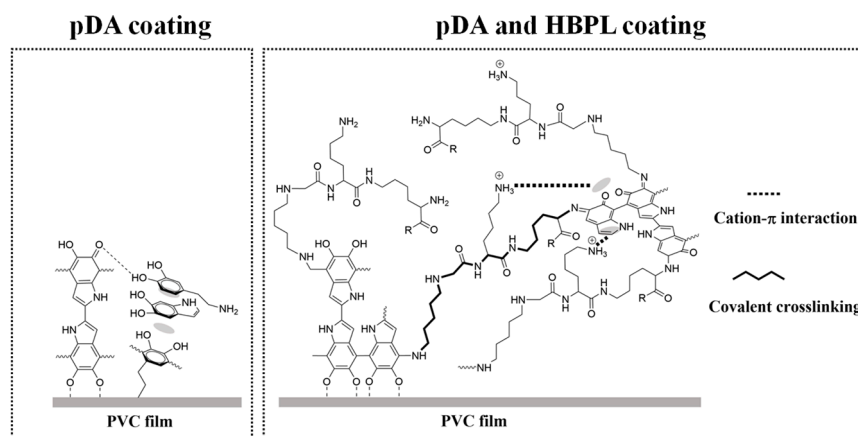


Figure 10. Schematic representation of interactions on PVC films with pDA and pDA/HBPL coatings.

4. Conclusions

Inspired by mussel adhesion protein, we coated polydopamine (pDA) onto the surface of PVC films in a weakly alkaline solution to form pDA particle aggregates. Additionally, a co-deposition and successive covalent-grafting process using a Schiff base reaction was employed to further incorporate HBPL into the coating. The addition of HBPL resulted in enhancement of the deposition amount and stability of pDA, particularly when the mass ratio of DA/HBPL was approximately 1:1. Simultaneously, the film's morphology exhibited increased roughness while the surface hydrophilicity significantly improved with the introduction of pDA and HBPL on its surface. Furthermore, the detachment of PVC-pDA/HBPL and PVC-pDA-HBPL was significantly reduced compared to that of PVC-pDA when the coatings were eluted with 1.0 M NaOH solutions, indicating enhanced stability under strongly basic conditions. Notably, the improvements were more pronounced for DA/HBPL co-deposition (PVC-pDA/HBPL) than for the successive deposition method involving PVC-pDA grafted with HBPL (PVC-pDA-HBPL), indicating that HBPL may act as a cross-linker during pDA deposition primarily through intermolecular Schiff base reactions, hydrogen bonding, or Michael addition. This marks the initial integration of

HBPL and dopamine for the hydrophilic modification of PVC materials, thereby broadening the scope of potential applications for PVC materials. This study presents a promising approach for the hydrophilic modification of PVC surfaces in biomedical applications due to its facile synthesis and incorporation of HBPL.

Author Contributions: Conceptualization, Y.Z., J.D. and L.W. (Liming Wang); methodology, Y.Z., D.W., Y.X. and L.W. (Li Wen); data curation, Y.Z., D.W., Y.X. and L.W. (Li Wen); investigation, Y.Z., J.D., L.W. (Li Wen) and D.W.; writing—review and editing, Y.Z., D.W. and J.D.; project administration, L.W. (Liming Wang) All authors have read and agreed to the published version of the manuscript.

Funding: This project was supported by the Youth Fund of Shaoxing University (No. 13011001002).

Institutional Review Board Statement: Not applicable.

Informed Consent Statement: Not applicable.

Data Availability Statement: Data are contained within the article.

Conflicts of Interest: Author Liming Wang was employed by the company Hisern Medical Equipment Co., Ltd. The remaining authors declare that the research was conducted in the absence of any commercial or financial relationships that could be construed as a potential conflict of interest.

References

1. Chiellini, F.; Ferri, M.; Morelli, A.; Dipaola, L.; Latini, G. Perspectives on alternatives to phthalate plasticized poly(vinyl chloride) in medical devices applications. *Prog. Polym. Sci.* **2013**, *38*, 1067–1088. [[CrossRef](#)]
2. Graham, J.; Keten, S. Increase in charge and density improves the strength and toughness of mussel foot protein 5 inspired protein materials. *ACS Biomater. Sci. Eng.* **2023**, *9*, 4662–4672. [[CrossRef](#)] [[PubMed](#)]
3. Kim, E.; Qin, X.; Qiao, J.; Zeng, Q.; Fortner, J.; Zhang, F. Graphene oxide/mussel foot protein composites for high-strength and ultra-tough thin films. *Sci. Rep.* **2020**, *10*, 19082. [[CrossRef](#)] [[PubMed](#)]
4. Aich, P.; An, J.; Yang, B.; Ko, Y.; Kim, J.; Murray, J.; Cha, H.; Roh, J.; Park, K.; Kim, K. Self-assembled adhesive biomaterials formed by a genetically designed fusion protein. *Chem. Commun.* **2018**, *54*, 12642–12645. [[CrossRef](#)] [[PubMed](#)]
5. Moulay, S. Dopa/catechol-tethered polymers: Bioadhesives and biomimetic adhesive materials. *J. Macromol. Sci. C* **2014**, *54*, 436–513. [[CrossRef](#)]
6. Lu, Q.; Danner, E.; Waite, J.; Israelachvili, J.; Zeng, H.; Hwang, D. Adhesion of mussel foot proteins to different substrate surfaces. *J. R. Soc. Interface* **2013**, *10*, 20120759. [[CrossRef](#)] [[PubMed](#)]
7. Lee, H.; Scherer, N.; Messersmith, P. Single-molecule mechanics of mussel adhesion. *Proc. Natl. Acad. Sci. USA* **2006**, *103*, 12999–13003. [[CrossRef](#)]
8. Han, J.; Zheng, S.; Jin, J.; Wu, T.; Shi, Y.; Yang, K.; Zhang, H.; Li, Y.; Sun, Y.; Lv, Y.; et al. Polydopamine-loaded prunetin nanomaterials activate DRD2 to reduce UV-induced inflammation by stabilizing and promoting Nrf2 nuclear translocation. *Acta Biomater.* **2023**, *169*, 556–565. [[CrossRef](#)]
9. Li, Y.; Yao, M.; Luo, Y.; Li, J.; Wang, Z.; Liang, C.; Qin, C.; Huang, C.; Yao, S. Polydopamine-reinforced hemicellulose-based multifunctional flexible hydrogels for human movement sensing and self-powered transdermal drug delivery. *ACS Appl. Mater. Interfaces* **2023**, *15*, 5883–5896. [[CrossRef](#)]
10. Li, L.; Xiong, W.; Wu, S.; Zhang, J. Ultrastable aluminum nanoparticles with enhanced combustion performance enabled by a polydopamine/polyethyleneimine nanocoating. *Langmuir* **2023**, *39*, 8833–8840. [[CrossRef](#)] [[PubMed](#)]
11. Gu, H.; Liu, Q.; Zhu, J.; Sun, G.; Liu, J.; Yu, J.; Li, R.; Li, Y.; Wang, J. Mussel-inspired polydopamine microspheres self-adhered on natural hemp fibers for marine uranium harvesting and photothermal-enhanced antifouling properties. *J. Colloid Interface Sci.* **2022**, *622*, 109–116. [[CrossRef](#)] [[PubMed](#)]
12. Asha, A.; Chen, Y.; Narain, R. Bioinspired dopamine and zwitterionic polymers for non-fouling surface engineering. *Chem. Soc. Rev.* **2021**, *50*, 11668–11683. [[CrossRef](#)] [[PubMed](#)]
13. Batul, R.; Tamanna, T.; Khaliq, A.; Yu, A. Recent progress in the biomedical applications of polydopamine nanostructures. *Biomater. Sci.* **2017**, *5*, 1204–1229. [[CrossRef](#)] [[PubMed](#)]
14. Hemmatpour, H.; De Luca, O.; Crestani, D.; Stuart, M.; Lasorsa, A.; van der Wel, P.; Loos, K.; Giousis, T.; Haddadi-Asl, V.; Rudolf, P. New insights in polydopamine formation via surface adsorption. *Nat. Commun.* **2023**, *14*, 664. [[CrossRef](#)] [[PubMed](#)]
15. Ho, C.; Ding, S. Structure, properties and applications of mussel-inspired polydopamine. *J. Biomed. Nanotechnol.* **2014**, *10*, 3063–3084. [[CrossRef](#)] [[PubMed](#)]
16. Ball, V. Polydopamine nanomaterials: Recent advances in synthesis methods and applications. *Front. Bioeng. Biotechnol.* **2018**, *6*, 109. [[CrossRef](#)]
17. Ball, V.; Hirtzel, J.; Leks, G.; Frisch, B.; Talon, I. Experimental methods to get polydopamine films: A comparative review on the synthesis methods, the films' composition and properties. *Macromol. Rapid Commun.* **2023**, *44*, e2200946. [[CrossRef](#)]

18. Li, H.; Jiang, B.; Li, J. Recent advances in dopamine-based materials constructed via one-pot co-assembly strategy. *Adv. Colloid Interface Sci.* **2021**, *295*, 102489. [[CrossRef](#)]
19. Geng, X.; Wang, J.; Ye, J.; Yang, S.; Han, Q.; Lin, H.; Liu, F. Electrospayed polydopamine membrane: Surface morphology, chemical stability and separation performance study. *Sep. Purif. Technol.* **2020**, *244*, 116857. [[CrossRef](#)]
20. Yang, W.; Liu, C.; Chen, Y. Stability of polydopamine coatings on gold substrates inspected by surface plasmon resonance imaging. *Langmuir* **2018**, *34*, 3565–3571. [[CrossRef](#)]
21. Wei, H.; Ren, J.; Han, B.; Xu, L.; Han, L.; Jia, L. Stability of polydopamine and poly (DOPA) melanin-like films on the surface of polymer membranes under strongly acidic and alkaline conditions. *Colloid Surface B* **2013**, *110*, 22–28. [[CrossRef](#)] [[PubMed](#)]
22. Yang, Y.; Qi, P.; Wen, F.; Li, X.; Xia, Q.; Maitz, M.; Yang, Z.; Shen, R.; Tu, Q.; Huang, N. Mussel-inspired one-step adherent coating rich in amine groups for covalent immobilization of heparin: Hemocompatibility, growth behaviors of vascular cells, and tissue response. *ACS Appl. Mater. Interfaces* **2014**, *6*, 14608–14620. [[CrossRef](#)] [[PubMed](#)]
23. Lee, H.; Lee, Y.; Statz, A.; Rho, J.; Park, T.; Messersmith, P. Substrate-independent layer-by-layer assembly by using mussel-adhesive-inspired polymers. *Adv. Mater.* **2008**, *20*, 1619–1623. [[CrossRef](#)] [[PubMed](#)]
24. Liu, Y.; Luo, R.; Shen, F.; Tang, L.; Wang, J.; Huang, N. Construction of mussel-inspired coating via the direct reaction of catechol and polyethyleneimine for efficient heparin immobilization. *Appl. Surf. Sci.* **2015**, *328*, 163–169. [[CrossRef](#)]
25. McGinty, K.; Brittain, W. Hydrophilic surface modification of poly (vinyl chloride) film and tubing using physisorbed free radical grafting technique. *Polymer* **2008**, *49*, 4350–4357. [[CrossRef](#)]
26. Yao, M.; Yan, Z.; Sun, X.; Guo, B.; Yu, C.; Zhao, Z.; Li, X.; Tan, Z.; Zhang, H.; Yao, F.; et al. Strongly adhesive zwitterionic composite hydrogel paints for surgical sutures and blood-contacting devices. *Acta Biomater.* **2023**, *166*, 201–211. [[CrossRef](#)] [[PubMed](#)]
27. Al-Ani, F.; Alsahy, Q.; Raheem, R.; Rashid, K.; Figoli, A. Experimental investigation of the effect of implanting TiO₂-NPs on PVC for long-term of membrane performance to treat refinery wastewater. *Membrane* **2020**, *10*, 77. [[CrossRef](#)] [[PubMed](#)]
28. Ahmad, T.; Liu, X.; Guria, C. Preparation of polyvinyl chloride (PVC) membrane blended with acrylamide grafted bentonite for oily water treatment. *Chemosphere* **2023**, *310*, 136840. [[CrossRef](#)]
29. Zhao, Y.; Kang, J.; Huang, W.; Kong, P.; An, D.; He, G. Copper nanowire/polydopamine-modified sodium alginate composite films with enhanced long-term stability and adhesion for flexible organic light-emitting diodes. *ACS Appl. Mater. Interfaces* **2023**, *15*, 52863–52873. [[CrossRef](#)]
30. Zhang, C.; Ou, Y.; Lei, W.; Wan, L.; Ji, J.; Xu, Z. CuSO₄/H₂O₂-induced rapid deposition of polydopamine coatings with high uniformity and enhanced stability. *Angew. Chem. Int. Edit.* **2016**, *55*, 3054–3057. [[CrossRef](#)]
31. Wei, Q.; Zhang, F.; Li, J.; Li, B.; Zhao, C. Oxidant-induced dopamine polymerization for multifunctional coatings. *Polym. Chem.* **2010**, *1*, 1430–1433. [[CrossRef](#)]
32. Zhang, W.; Liao, Z.; Meng, X.; Niwaer, A.; Wang, H.; Li, X.; Liu, D.; Zuo, F. Fast coating of hydrophobic upconversion nanoparticles by NaIO₄-induced polymerization of dopamine: Positively charged surfaces and in situ deposition of Au nanoparticles. *Appl. Surf. Sci.* **2020**, *527*, 146821. [[CrossRef](#)]
33. Wu, M.; Liu, J.; Wang, X.; Zeng, H. Recent advances in antimicrobial surfaces via tunable molecular interactions: Nanoarchitectonics and bioengineering applications. *Curr. Opin. Colloid Interface Sci.* **2023**, *66*, 101707. [[CrossRef](#)]
34. Yang, Z.; Xi, Y.; Bai, J.; Jiang, Z.; Wang, S.; Zhang, H.; Dai, W.; Chen, C.; Gou, Z.; Yang, G.; et al. Covalent grafting of hyperbranched poly-L-lysine on Ti-based implants achieves dual functions of antibacteria and promoted osteointegration in vivo. *Biomaterials* **2021**, *269*, 120534. [[CrossRef](#)] [[PubMed](#)]
35. Song, B.; Park, I.; Park, D.; Kim, Y.; Kim, M.; Lee, K.; Park, S.; Choi, B.; Min, B. Anti-adhesive effect of chondrocyte-derived extracellular matrix surface-modified with poly-L-lysine. *J. Tissue Eng. Regen. Med.* **2022**, *16*, 279–289. [[CrossRef](#)]
36. Yuan, Y.; Shi, X.; Gan, Z.; Wang, F. Modification of porous PLGA microspheres by poly-L-lysine for use as tissue engineering scaffolds. *Colloid Surface B* **2017**, *161*, 162–168. [[CrossRef](#)]
37. Wang, J.; Sun, Y.; Liu, X.; Kang, Y.; Cao, W.; Ye, J.; Gao, C. An antibacterial and anti-oxidant hydrogel containing hyperbranched poly-L-lysine and tea polyphenols accelerates healing of infected wound. *Biomater. Adv.* **2023**, *157*, 213755. [[CrossRef](#)] [[PubMed](#)]
38. Tu, C.; Lu, H.; Zhou, T.; Zhang, W.; Deng, L.; Cao, W.; Yang, Z.; Wang, Z.; Wu, X.; Ding, J.; et al. Promoting the healing of infected diabetic wound by an anti-bacterial and nano-enzyme-containing hydrogel with inflammation-suppressing, ROS-scavenging, oxygen and nitric oxide-generating properties. *Biomaterials* **2022**, *286*, 121597. [[CrossRef](#)]
39. Li, C.; Yang, Q.; Chen, D.; Zhu, H.; Chen, J.; Liu, R.; Dang, Q.; Wang, X. Polyethyleneimine-assisted co-deposition of polydopamine coating with enhanced stability and efficient secondary modification. *RSC Adv.* **2022**, *12*, 35051–35063. [[CrossRef](#)]
40. Chen, R.; Lin, B.; Luo, R. Recent progress in polydopamine-based composites for the adsorption and degradation of industrial wastewater treatment. *Heliyon* **2022**, *8*, e12105. [[CrossRef](#)]
41. Tsai, M.; Chang, M.; Chien, H. Effect of codeposition of polydopamine with polyethylenimine or poly(ethylene glycol) coatings on silver nanoparticle synthesis. *Langmuir* **2023**, *39*, 6895–6904. [[CrossRef](#)] [[PubMed](#)]
42. Cihanoğlu, A.; Schiffman, J.; Alsoy Altinkaya, S. Biofouling-resistant ultrafiltration membranes via codeposition of dopamine and cetyltrimethylammonium bromide with retained size selectivity and water flux. *ACS Appl. Mater. Interfaces* **2022**, *14*, 38116–38131. [[CrossRef](#)]
43. Cai, H.; Wang, Y.; Wu, K.; Guo, W. Enhanced hydrophilic and electrophilic properties of polyvinyl chloride (PVC) biofilm carrier. *Polymers* **2020**, *12*, 1240. [[CrossRef](#)] [[PubMed](#)]

44. Kazmierska, K.; Szwast, M.; Ciach, T. Determination of urethral catheter surface lubricity. *J. Mater. Sci.-Mater. M.* **2008**, *19*, 2301–2306. [[CrossRef](#)] [[PubMed](#)]
45. Tapia-Lopez, L.; Luna-Velasco, M.; Beaven, E.; Conejo-Dávila, A.; Nurunnabi, M.; Castro, J. RGD peptide-functionalized polyether ether ketone surface improves biocompatibility and cell response. *ACS Biomater. Sci. Eng.* **2023**, *9*, 5270–5278. [[CrossRef](#)]
46. Qiu, W.; Yang, H.; Xu, Z. Dopamine-assisted co-deposition: An emerging and promising strategy for surface modification. *Adv. Colloid Interface* **2018**, *256*, 111–125. [[CrossRef](#)]
47. Yao, L.; He, C.; Chen, S.; Zhao, W.; Xie, Y.; Sun, S.; Nie, S.; Zhao, C. Codeposition of polydopamine and zwitterionic polymer on membrane surface with enhanced stability and antibiofouling property. *Langmuir* **2019**, *35*, 1430–1439. [[CrossRef](#)]

Disclaimer/Publisher’s Note: The statements, opinions and data contained in all publications are solely those of the individual author(s) and contributor(s) and not of MDPI and/or the editor(s). MDPI and/or the editor(s) disclaim responsibility for any injury to people or property resulting from any ideas, methods, instructions or products referred to in the content.